MADRID
inter.noise 2019
June 16 - 19
NOISE CONTROL FOR A BETTER ENVIRONMENT

Control of Aeroacoustic Noise Generation during Flow Past a Circular Cylinder using Splitter Plate

Mahato, Bikash[1]

Ganta, Naveen[2]

Bhumkar, Yogesh G.[3]

Scientific Computing Laboratory, School of Mechanical Sciences
Indian Institute of Technology Bhubaneswar

ABSTRACT

Aeolian tone generation during unsteady, two-dimensional flow past a circular cylinder in the presence of splitter plates has been numerically investigated at Reynolds number $Re = 150$ and Mach number $M = 0.2$ using direct numerical simulations (DNS). Computations have been performed for flow over a circular cylinder with and without splitter plates. Arc shaped splitter plates have been placed near the top surface of the cylinder. Compressible Navier-Stokes equations in non-dimensional form have been solved using combination of optimized coupled compact difference (OCCD) scheme and optimized five stage Runge-Kutta $(ORK5)$ time integration scheme. O-grid topology has been adopted in the present computations to generate refined mesh inside computational domain. Computational domain has been divided into acoustic and buffer zones. Acoustic zone covers up to $100D$ radius with closely spaced grid points, where, D is the diameter of cylinder. On the other hand, buffer zone has comparatively coarser grid, which helps to dissipate high wavenumber numerical oscillations generated during calculations and thereby avoiding reflections from the outer boundary. Results show amplitudes of fluctuating lift forces are reduced in the presence of splitter plate. Placing the splitter plate near the top surface of cylinder resulted in changes in vorticity contours and delay in flow separation. Due to this reason, mean drag has been decrease on the cylinder in the presence of splitter plates. Disturbance pressure field shows less intensity for the case with splitter plate than without splitter plate. Directivity patterns based on root mean square (RMS) values of disturbance pressure have also shown that there is a reduction in net acoustic noise radiated from cylinder with splitter plate. Furthermore, acoustic, thermal and hydrodynamic modes have been decomposed using Doak's decomposition theory.

[1]bm18@iitbbs.ac.in
[2]ng13@iitbbs.ac.in
[3]bhumkar@iitbbs.ac.in

Acoustic modes have confirmed that the net acoustic noise has been reduced by placing the splitter plate. Approximated Lighthill source term has been evaluated to understand distribution of noise source terms.

Keywords: Splitter plate, Aeolian tone, Approximated Lighthill's noise source
I-INCE Classification of Subject Number: 20
(see http://i-ince.org/files/data/classification.pdf)

1. INTRODUCTION

Flow and acoustic control from bluff bodies is one of interesting topics among the researchers during the last few decades. Researcher have tried to modify flow and acoustics by either changing original object geometry or by attaching additional body parts near the original geometry. Control of flow and acoustic signature radiated from bluff bodies involves understanding of how vortices are forms and the way they interact with each other. Study on bluff body flow gives rich flow physics to analyze and understand the behavior of wakes, fluid-structure interactions and vortex induced vibrations. Bluff body dynamics has many applications in aerospace as well as in constructions.

Famous work on aeolian tone by Strouhal [1] gives rise in interests on many researcher. Relation between free-stream fluid velocity and frequency of the generated sound field has first proposed by Strouhal and that has been expressed as Strouhal number, $St = \frac{fD}{U_\infty}$. Many investigators have measured and compared the laminar vortex shedding frequency, Strouhal number at low Reynolds numbers [2, 3, 4]. Flow modification by inserting additional objects near bluff body has been first successfully experimented by Roshko [5]. Mathematical model for sound propagation in open domain has been presented in the famous work of Lighthill [6].

In this present simulation, unsteady flow past an circular cylinder and cylinder with splitter plate have been considered. Splitter plate is kept near the top surface of the cylinder. Computations have been performed at Reynolds number, $Re = 150$. Obtained flow physics and acoustics properties have been analyzed to understand the effects of splitter plates. The obtained *DNS* flow fields have been further decomposed into hydrodynamic, acoustic and thermal modes using Doak's decomposition theory [7, 8] for better understanding of flow field properties. Approximated Lighthill's source model technique has been used to identify the noise sources presents in the solution.

2. PROBLEM DEFINITION

Schematic of present problem has been shown in Fig. 1. Non-dimensional diameter of cylinder has been taken as 1. Splitter plate of curvy in shape has been placed near the top surface of a circular cylinder. Plate is being placed at a non-dimensional radius of R_{Plate} ($= 0.735$) from the cylinder center as shown in schematic. The splitter plates arc angle has been taken as 10^o. Nine different angular positions (θ, as mentioned in schematic) of the splitter plate has been consider for present calculation. Minimum and maximum angular position has been taken as 65^o and 105^o, respectively with an increment of 5^o (65^o, 70^o, 75^o, 80^o, 85^o, 90^o, 95^o, 100^o, and 105^o). Arc length of the splitter plate is fixed as 10^o for all the cases. Cylinder and splitter plate assembly has been placed inside an uniform free-stream velocity, U_∞. Reynolds number, Re ($= \frac{\rho U_\infty D}{\nu}$, D is diameter of the

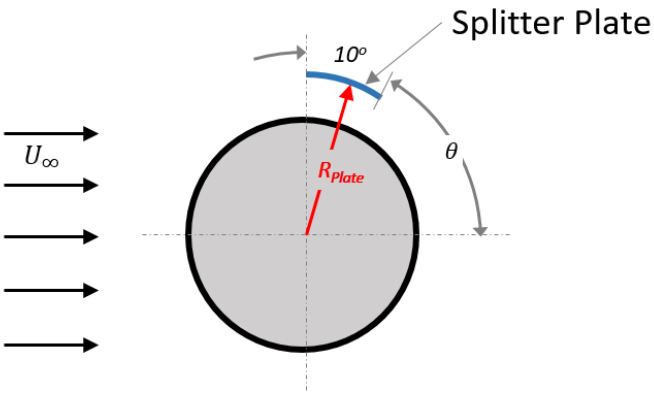

Figure 1: Schematic of cylinder with splitter plate attachment.

cylinder) and Mach number has been considered as 150 and 0.2, respectively . Other fluid properties like density, temperature etc. are considered as air properties at 25^oC.

3. NUMERICAL DOMAIN AND METHOD

O-shaped topology structured grid of $1500D$ outer diameter has been considered in this calculation. 501 and 900 grid points have been taken in azimuthal and radial direction, respectively. Computational domain has been divided into acoustic zone and buffer zone. Acoustic zone has been considered till $r = 100D$, where r is the radial distance from cylinder center. Within the acoustic zone, $\sim$ 724 grid points has been closely placed, so that high frequency acoustic waves are accurately gets resolved. Rest of the domain has been considered as buffer zone. Buffer zone consists of coarser grid points as compared to acoustic zone, so that the high frequency numerical disturbances get dissipated over distance.

Unsteady compressible Navier-stokes equations have been solved to calculate flow properties inside to computational domain [9]. Physical domain equations have been transformed into equispaced computational domain so that compact finite difference scheme can be easily implemented. A high accurate Optimized Couple Compact Difference ($OCCD$) scheme [10] has been used for space derivatives presents in the transformed equations except for viscous derivatives. Viscous derivatives are calculated using traditional second order central difference scheme. Temporal derivatives has been calculated using Optimized five-stage Runge-Kutta ($ORK5$) [11] time integration method. No-slip and characteristics based boundary conditions have been implemented on the walls and at the outer boundary, respectively.

3.3.1. Position of splitter plate

Effect of angular positions of splitter plate has been studied in this analysis by keeping radial distance fixed. Different angular positions varying from 65^o to 105^o with an increment of 5^o have been considered for the calculations. Effect of different radial distance of splitter plate has not been shown in this manuscript. We have performed the analysis for different radial distance of splitter plate and radial distance, $R_{Plate} = 0.735$ has been found to be most effective for Mach number 0.2 and Reynolds number 150. So, for this analysis radial distance of the splitter plate has been fixed at, $R_{Plate} = 0.735$.

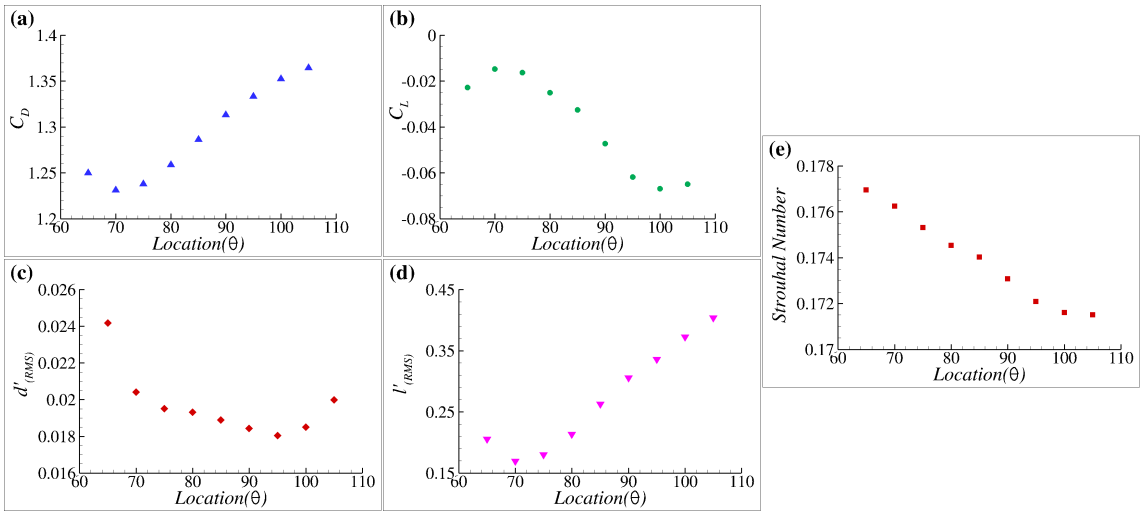

Figure 2: Mean and disturbance of flow properties.

4. RESULTS AND DISCUSSIONS

Flow and acoustic properties obtained from numerical analysis have been presented in this section. Flow simulations have been allowed to performed for sufficient time so that the solutions will reach its time steady state. Flow and acoustic properties for the present problem have been evaluated based on the time stationary flow field data. All instantaneous plots shown in this manuscript are taken at maximum lift condition.

4.4.1. Flow properties

Mean and fluctuating properties of the present simulations have been presented in Fig. 2. Figure 2(a) and (b) shows the mean drag (C_D) and lift (C_L) coefficient for different angular positions. From these two figure it has been seen that at $\theta = 70^o$ both drag and lift is minimum compare to other cases. Figure 2(c) and (d) represents root mean square (RMS) quantity of drag ($d'_{(RMS)}$) and lift ($l'_{(RMS)}$) fluctuations. Angular position $\theta = 70^o$ show minimum lift fluctuation and $\theta = 95^o$ show minimum drag fluctuation compare to other angular positions. Strouhal number plot at Fig. 2(e) shown a decreasing trend of vortex shedding frequency as we are moving splitter plate position towards the upstream direction.

Although we have performed simulations for all different angular positions, but most of the comparisons have been shown after this paragraph are between cylinder without-splitter-plate and with-splitter-plate attached at $\theta = 70^o$ position. The reason for choosing this particular position is because, placing splitter plate at $\theta = 70^o$ angular position shows maximum reduction in drag force as well as minimum value of RMS lift fluctuation ($l'_{(RMS)}$) as shown in Fig. 2(d). Wherever in this manuscript the angular position of the splitter plate is not mentioned, reader has to assume that the plate has been placed at $\theta = 70^o$ angular position.

Figure 3(a) and (b) shows changes of lift and drag fluctuation due to the presence of splitter plate. Figure 3(c) and (d) shows the frequency presents in the lift and drag oscillations. Fourier transformation of lift and drag force has been plotted in Fig. 3(c) and (d). Fig. 3(c) and (d) shows that frequency of drag fluctuation has increased with the insertion of splitter plate. Before insertion of splitter plate, drag force oscillating frequency is twice as lift frequency, but due to presence of splitter plate drag and lift

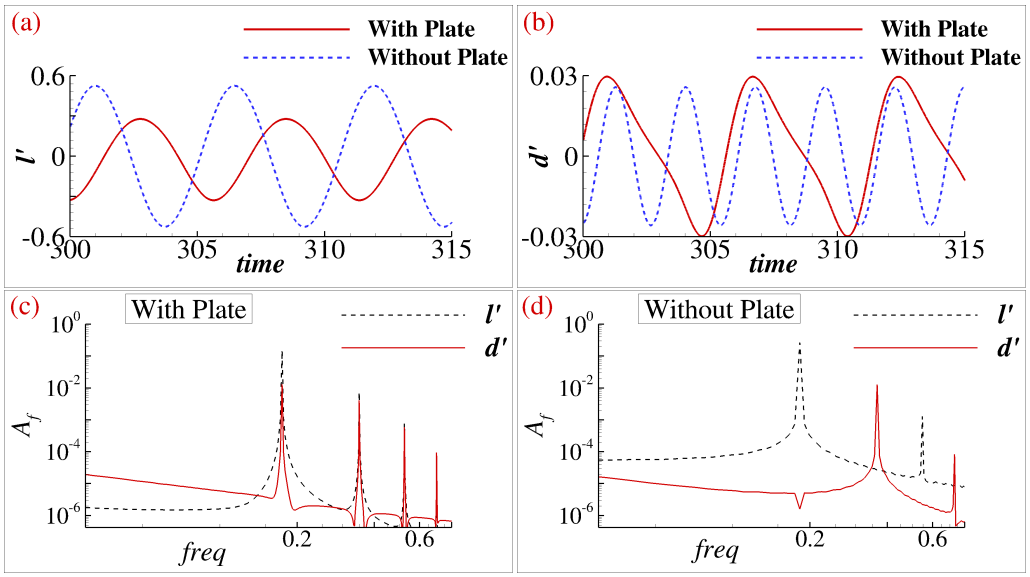

Figure 3: Lift and drag fluctuation varying with time.

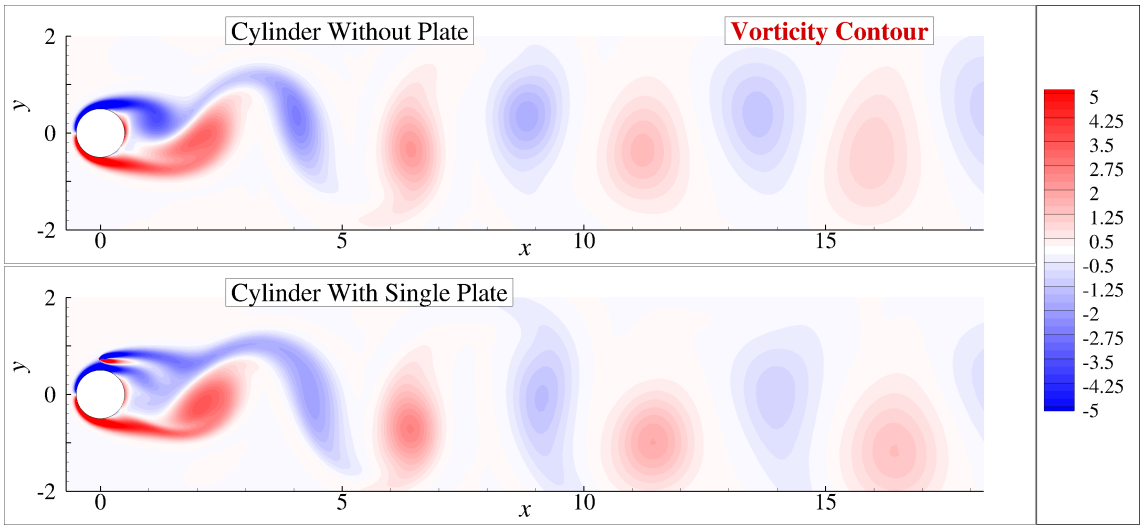

Figure 4: Vorticity contour.

frequency become equal. Similar observation also can be seen in time varying drag fluctuation plot in Fig. 3(b).

Figure 4 shows instantaneous vorticity contour at maximum lift condition. Insertion of splitter plat near the top surface of the cylinder creates opposite vorticity which leads to reduction in vorticity of vortices generated from top surfaces. Along with that splitter plate guided some high momentum fluids into the wake region, this leads to delay in flow separation at the top surface. Hence, with-plate cylinder observe lesser drag compare to cylinder without-plate.

4.4.2. Acoustic properties

Disturbance pressure fields have been calculated by subtracting mean pressure from instantaneous pressure field data. Pressure disturbance fields have been compared between without-plate and with-plate cylinder and the comparison has been shown in Fig. 5. 41 equi-spaced contour level has been used in this figure with minimum and

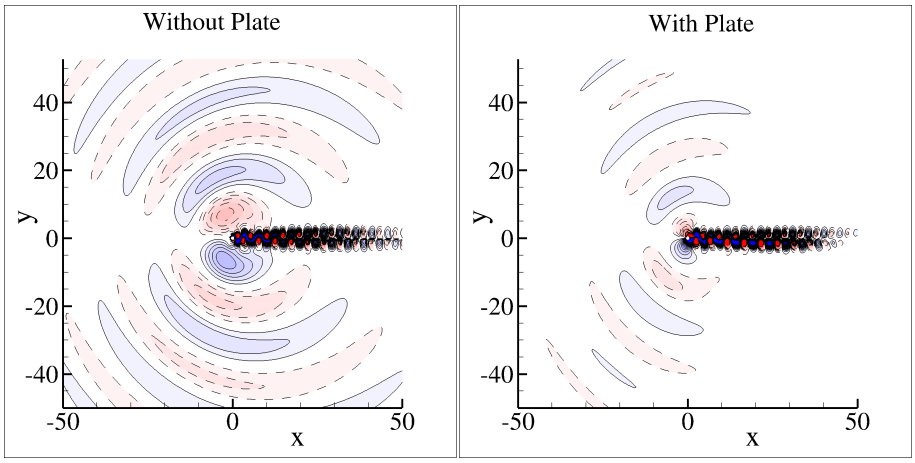

Figure 5: Disturbance pressure propagation with and without plate.

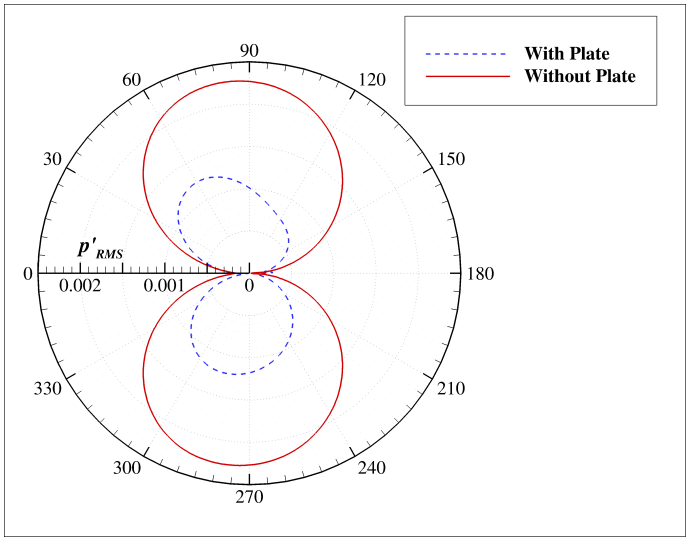

Figure 6: RMS of time mean pressure fluctuation at radius of 75.

maximum contour value of -0.4 and 0.4, respectively. Pressure fluctuation contour plot shows significant reduction in disturbance pressure in the presence of splitter plate.

RMS of pressure fluctuation has been calculated by considering 10 complete lift cycle fluctuation value. RMS plot shows that acoustic disturbances is reduced significantly after insertion of splitter plate. One important observation from this plot is, even after placing single plate on the top side of the cylinder, acoustic radiation reduced in both top and bottom side. More on this has been discussed in the 4.4 section.

Acoustic power has been calculated by integrating $p'_{(RMS)}$ at a radial distance of 75 from circular cylinder. Mathematically,

$$Acoustic\ Power = 20 \log 10 \left(\frac{\tilde{p}}{p_0} \right) \tag{1}$$

here, $\tilde{p} = \int_{\pi}^{2\pi} p'_{RMS}|_{r=75}\, d\theta$ and p_0 is reference pressure. For these calculations, p_0 has been taken as acoustic power of cylinder without-splitter plate attached. Acoustic power plot (Fig. 7) also shows minimum acoustic radiation when plate has been kept at $\theta = 70^o$.

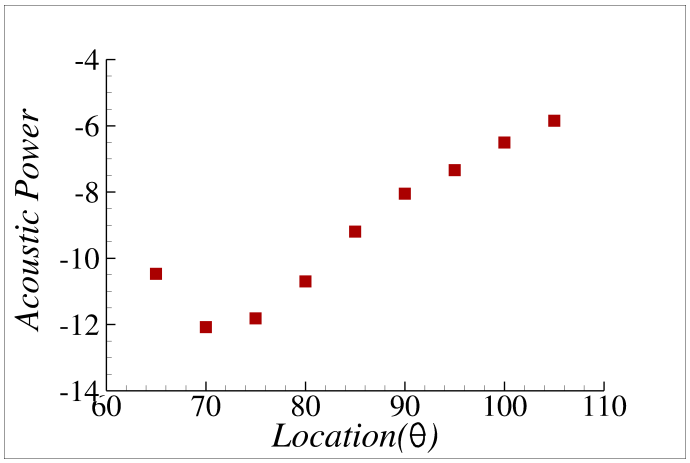

Figure 7: Acoustic power for all splitter plate positions.

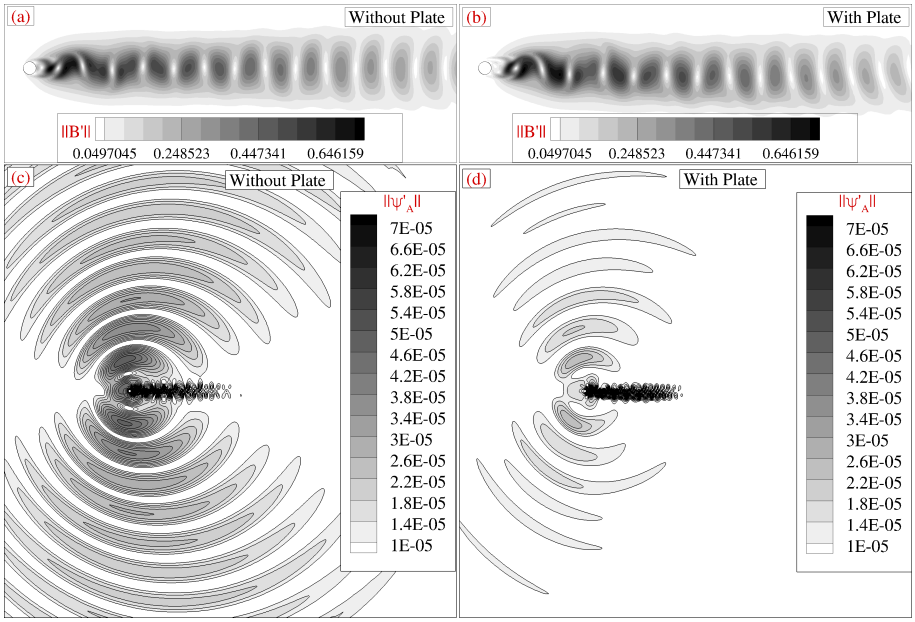

Figure 8: Hydrodynamic and acoustic disturbances with and without splitter plate.

4.4.3. Doaks decomposition

Momentum density ($\rho\mathbf{u}$) field has been decomposed into hydrodynamic, acoustic and thermal modes [8] to get better insight of flow physics. Decomposition has been obtained by applying Doak's decomposition theory [7]. The momentum density field has been decomposed into solenoidal and irrotational components. Fluctuating solenoidal component represents vortical disturbance intensity, and irrotational field represents combination of thermal and acoustic component. Instantaneous fluctuating solenoidal components (B'), *i.e.* hydrodynamic mode has been shown in Fig. 8(a) and (b). Hydrodynamic component is not showing much difference in the presence of splitter plate. Acoustic mode (ψ'_A) comparison, *i.e.* extracted acoustic field from irrotational component of momentum density field has been shown in Fig. 8(c) and (d). Acoustic mode shows significant reduction in amplitude in the presence of splitter plate and there is slight difference between directivity at the top and the bottom side.

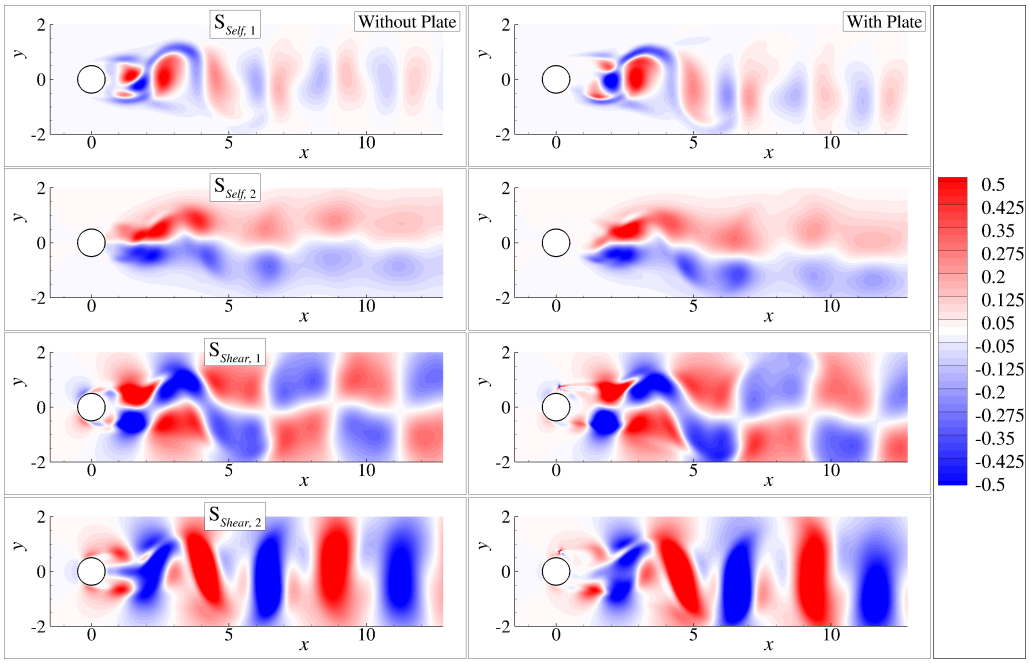

Figure 9: Approximated Lighthill's source term comparison.

4.4.4. Approximated Lighthill's Analogy

Cheong *et al*. in their research article [17] approximated Lighthill's stress term as the self noise and shear noise source term by assuming that the viscous stress and the entropy fluctuations are negligible within the moving fluid. The Lighthill source term has been approximated as mentioned in Eq. (2). First term in the right hand side represent self noise source and second and third together represents shear noise source. Last term only contains mean velocity components and hence does not contribute in sound generation.

$$S_{ALST,\,i} = -\frac{\partial \rho u_i' u_j'}{\partial x_j} - \frac{\partial \rho u_i' \bar{u}_j}{\partial x_j} - \frac{\partial \rho \bar{u}_i u_j'}{\partial x_j} - \frac{\partial \rho \bar{u}_i \bar{u}_j}{\partial x_j} \tag{2}$$

Self and shear noise terms have been calculated and shown in Fig. 9. Left column figures represents source terms without-splitter plate and right column figures represent sources with-splitter plate. Here, all source terms shown in this figure shows shifting of maximum intensity toward downstream direction in presence of splitter plate. This is because of, generation and intensity of noise sources are depends on way of interaction between vortices, in this case, one is generated from top surface another is generated from the bottom surface and they interact in the wake region. As we are disturbing the top vortex, vorticity of the top vortex is reduced and at the same time it distributes in larger area. This prevents noise generation near to the top surface of the cylinder. So, the overall intensity of noise source terms have been reduced after insertion of splitter plate. Similar observation has been seen in p'_{RMS} plot shown in Fig. 6.

5. CONCLUSIONS

Computations have been performed for flow past circular cylinder in presence of splitter plate using high accuracy *DRP* spatial discretization scheme and five-stage Runge-Kutta time integration scheme. Flow physics have been analyzed for different

splitter plate positions. Among the all other angular positions of splitter plate, at $\theta = 70^o$ fluid exerts minimum lift and drag force on the cylinder. Pressure fluctuation is also minimum for this case. Acoustic power plot show insertion of splitter plate helps to significantly reduce noise emission due to flow over the cylinder. Reduction in noise generation and propagation has been shown with the help of Doak's decomposition technique and approximated Lighthill's source terms. From the above numerical experiments, $\theta = 70^o$ is the best position found for reducing noise generated due to fluid flow as well as reducing drag force exerted on the cylinder.

6. REFERENCES

[1] Vinzenz Strouhal. Über eine besondere art der tonerregung. *Annalen der Physik*, 241(10):216–251, 1878.

[2] H Oertel Jr. Wakes behind blunt bodies. *Annual Review of Fluid Mechanics*, 22(1):539–562, 1990.

[3] McGranahan B. D. Broughton B. A. Deters R. W. Brandt J. B. Williamson, G. A. and M. S. Selig. Summary of low-speed airfoil data. 5, 2012.

[4] Osamu Inoue and Nozomu Hatakeyama. Sound generation by a two-dimensional circular cylinder in a uniform flow. *Journal of Fluid Mechanics*, 471:285–314, 2002.

[5] Anatol Roshko. On the drag and shedding frequency of two-dimensional bluff bodies. 1954.

[6] Michael James Lighthill. On sound generated aerodynamically I. general theory. *Proceedings of the Royal Society of London. Series A. Mathematical and Physical Sciences*, 211(1107):564–587, 1952.

[7] PE Doak. Momentum potential theory of energy flux carried by momentum fluctuations. *Journal of sound and vibration*, 131(1):67–90, 1989.

[8] S Unnikrishnan and Datta V Gaitonde. Acoustic, hydrodynamic and thermal modes in a supersonic cold jet. *Journal of Fluid Mechanics*, 800:387–432, 2016.

[9] K. A. Hoffman and T. C. Steve. *Computational Fluid Dynamics Volume I & II.* Engineering Education System, 2000.

[10] Bikash Mahato, Naveen Ganta, and Yogesh G Bhumkar. Direct simulation of sound generation by a two-dimensional flow past a wedge. *Physics of Fluids*, 30(9):096101, 2018.

[11] Jitenjaya Pradhan, Saksham Jindal, Bikash Mahato, and Yogesh G Bhumkar. Joint optimization of the spatial and the temporal discretization scheme for accurate computation of acoustic problems. *Commun. Comput. Phys*, 24:408–434, 2018.

[12] JE Ffowcs Williams. Aeroacoustics. *Annual Review of Fluid Mechanics*, 9(1):447–468, 1977.

[13] JE Ffowcs Williams. Hydrodynamic noise. *Annual Review of Fluid Mechanics*, 1(1):197–222, 1969.

[14] John William Strutt and Baron Rayleigh. *The theory of sound*. Dover, 1945.

[15] JH Gerrard. Measurements of the sound from circular cylinders in an air stream. *Proceedings of the Physical Society. Section B*, 68(7):453, 1955.

[16] Bikash Mahato, Ganta Naveen, and Yogesh G Bhumkar. Computation of aeroacoustics and fluid flow problems using a novel dispersion relation preserving scheme. *Journal of Theoretical and Computational Acoustics*, 26(4):1850063, 2019.

[17] Cheolung Cheong, Phillip Joseph, Yonghwan Park, and Soogab Lee. Computation of aeolian tone from a circular cylinder using source models. *Applied Acoustics*, 69(2):110–126, 2008.